Hierarchical Porous Materials | Hot Paper

International Edition: DOI: 10.1002/anie.201506391
German Edition: DOI: 10.1002/ange.201506391

Hydrolytic Transformation of Microporous Metal–Organic Frameworks to Hierarchical Micro- and Mesoporous MOFs

*Yonghwi Kim, Tao Yang, Gyeongwon Yun, Mohammad Bagher Ghasemian, Jaehyoung Koo, Eunsung Lee, Sung June Cho, and Kimoon Kim**

Dedicated to Professor James A. Ibers on the occasion of his 85th birthday

Abstract: *A new approach to the synthesis of hierarchical micro- and mesoporous MOFs from microporous MOFs involves a simple hydrolytic post-synthetic procedure. As a proof of concept, a new microporous MOF, POST-66(Y), was synthesized and its transformation into a hierarchical micro- and mesoporous MOF by water treatment was studied. This method produced mesopores in the range of 3 to 20 nm in the MOF while maintaining the original microporous structure, at least in part. The degree of micro- and mesoporosity can be controlled by adjusting the time and temperature of hydrolysis. The resulting hierarchical porous MOF, POST-66(Y)-wt, can be utilized to encapsulate nanometer-sized guests such as proteins, and the enhanced stability and recyclability of an encapsulated enzyme is demonstrated.*

Metal–organic frameworks (MOFs) constructed from metal ions (or clusters) and organic ligands by self-assembly are an important class of synthetic porous materials. Thanks to their well-defined pore structures with high surface areas, MOFs have been extensively studied for various applications, such as gas sorption, separation, catalysis, and drug delivery.[1–5] As the properties and functions of MOFs are often dictated by the size and shape of pores in MOFs, tremendous efforts have been made to control the size of pores in MOFs.[6] However, the pores of most MOFs belong to the micropore regime (less than 2 nm) and only a few mesoporous MOFs have been reported.[7] Furthermore, most mesoporous MOFs prepared by conventional solvothermal synthesis have pore sizes smaller than 5 nm. Recently, considerable efforts have been devoted to the creation of mesopores of more than 5 nm in MOFs.[8] So far, such mesoporous MOFs are produced by direct synthetic methods, including ligand extension, template-assisted synthesis, and imperfect crystallization (defect formation).[9–12] Since these methods require rather elaborated synthetic procedures, it is highly desirable to develop a simple and reliable method to produce mesoporous MOFs. Furthermore, porous materials having both micro- and mesopores are expected to be useful for many practical applications, but the synthesis of MOFs with such hierarchical pore structures in a controlled manner is still challenging.

Recently, we and others investigated the post-synthetic modification of MOFs,[13] especially post-synthetic substitution of metal ions or ligands in MOFs.[14] Based on these studies, we envisioned that partial removal of metal ions and/or ligands of microporous MOFs may generate larger pores while maintaining the original microporosity, at least in part (Scheme 1), to produce hierarchical MOFs with micro- and mesoporosity. Although partial desilication or dealumination has been used to produce hierarchical structures in zeolites,[15] little attention has been paid to the generation of mesopores by partial dissolution of microporous MOFs.[16] Herein, we report a new approach to the synthesis of hierarchical micro- and mesoporous MOFs from microporous MOFs by a simple hydrolytic post-synthetic procedure. As a proof of concept, we synthesized a new microporous MOF, POST-66(Y), and studied its transformation into a hierarchical micro- and mesoporous MOF by simple water treatment. Encapsulation of an enzyme in the resulting hierarchical MOF with enhanced enzyme stability and recyclability is also demonstrated.

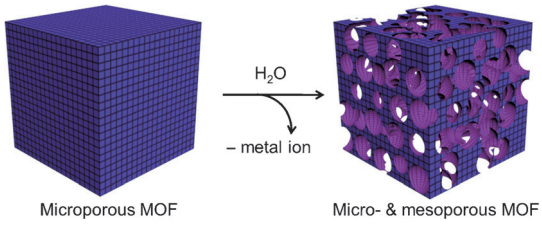

Scheme 1. View of hydrolytic post-synthetic transformation in a MOF, resulting in larger pores by partial removal of constituents.

[*] Dr. Y. Kim, Dr. T. Yang, Dr. G. Yun, M. B. Ghasemian, J. Koo, Prof. Dr. E. Lee, Prof. Dr. K. Kim
Center for Self-assembly and Complexity (CSC)
Institute for Basic Science (IBS)
Pohang, 790-784 (Republic of Korea)
E-mail: kkim@postech.ac.kr
Homepage: http://csc.ibs.re.kr/
J. Koo, Prof. Dr. E. Lee, Prof. Dr. K. Kim
Department of Chemistry
Pohang University of Science and Technology
Pohang, 790-784 (Republic of Korea)
Prof. Dr. K. Kim
Division of Advanced Materials Science
Pohang University of Science and Technology
Pohang, 790-784 (Republic of Korea)
Prof. Dr. S. J. Cho
Department of Chemical Engineering, Chonnam National University
Gwangju, 500-757 (Republic of Korea)

Supporting information for this article is available on the WWW under http://dx.doi.org/10.1002/anie.201506391.

Colorless truncated octahedron-shaped crystals of the new MOF POST-66(Y) were synthesized by a solvothermal reaction of $Y(NO_3)_3{\cdot}5H_2O$ with H_3hmtt (methyl substituted truxene tricarboxylic acid; Figure 1a) in a mixture of DMF, methanol, and water.[14b] The chemical formula of POST-66(Y), $[\{Y_4(H_2O)\}_3(hmtt)_8](OH)_6(NO_3)_6{\cdot}70\,DMF{\cdot}67\,H_2O$, was determined by X-ray crystallography, elemental analysis (EA), thermogravimetric analysis (TGA), and NMR spectroscopy (Supporting Information, Figures S1, S2). Single-crystal X-ray diffraction analysis revealed that POST-66(Y) crystallizes in the space group $Fm\bar{3}c$ and consists of $\{Y_4(H_2O)\}^{12+}$ as secondary building units (SBUs) and $hmtt^{3-}$ as a linker. The Y^{3+} ions of H_2O-centered square-planar $\{Y_4(H_2O)\}^{12+}$ units are connected through the carboxylates from eight surrounding $hmtt^{3-}$ ligands (Figure 1b). In turn, each triangular $hmtt^{3-}$ ligand is connected to three $\{Y_4(H_2O)\}^{12+}$ squares to generate an uninodal 8-connected **reo** net (Figure 1c).[17] A basic building unit for the structure is an octahedral cage consisting of six $\{Y_4(H_2O)\}^{12+}$ squares and eight $hmtt^{3-}$ ligands (Figure 1d). Each octahedral cage shares vertices with others to generate an infinite network structure with additional cuboctahedral cages (Figure 1e). The positive charge (+12 per formula unit) of the framework is balanced by hydroxide and nitrate ions, suggested by elemental analysis (EA). POST-66(Y) possesses considerable void space (71% of the unit cell volume) as well as low density of 0.58 $g\,cm^{-3}$ owing to the large octahedral and cuboctahedral cages.[18] The interconnected cuboctahedral cages form three-dimensional open channels with an aperture of 1.3 nm diameter (Supporting Information, Figure S3).

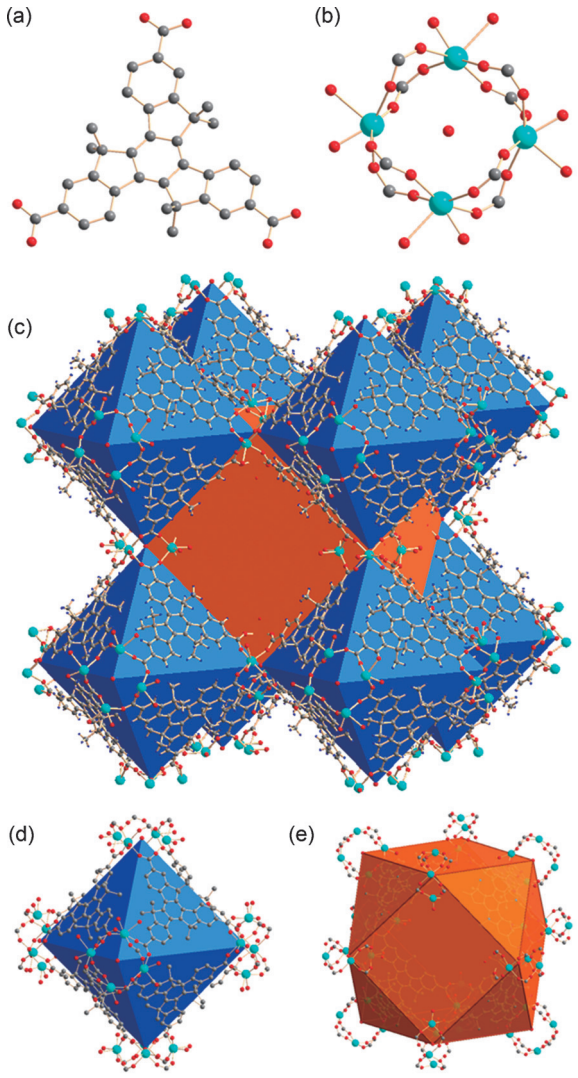

Figure 1. a) Structure of hmtt, b) SBU of POST-66, c) crystal structure of POST-66, d) octahedral cage, and e) cuboctahedral cage.

POST-66(Y) showed high thermal stability (>350 °C; Supporting Information, Figure S4) and permanent porosity after evacuation of solvent molecules. N_2 sorption data of POST-66(Y) at 77 K showed a type I isotherm with a secondary uptake before $P/P_0 = 0.1$ suggesting the presence of two kinds of micropores (Figure 2a).[19] No hysteresis was observed during the desorption. The sorption isotherm was fitted to a BET equation, which gave a surface area of 2400 $m^2\,g^{-1}$ and a total specific pore volume of 0.89 $cm^3\,g^{-1}$.

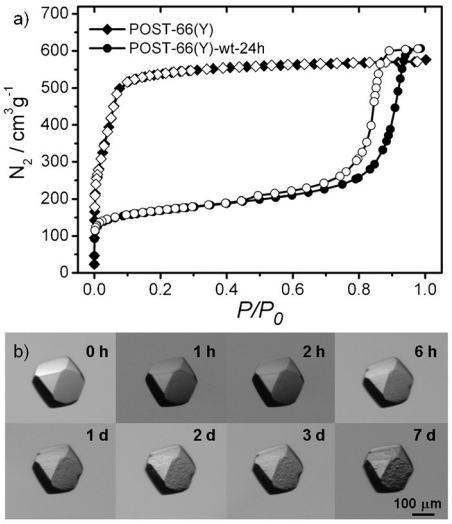

Figure 2. a) N_2 sorption isotherms of as prepared POST-66(Y) and POST-66(Y)-wt-24h, b) Photographs of POST-66(Y) crystal after soaking in water.

Many MOFs are known to be unstable in water, as water molecules can easily bind to metal ions and induce destruction of MOFs by removal of the metal ions through substitution or hydrolysis.[20] We therefore decided to explore water as a dissolution agent to create additional mesopores in microporous MOF (Scheme 1). To induce mesopores in the framework, crystals of POST-66(Y) were immersed in water at room temperature for 24 h. Although the water-treated crystals (POST-66(Y)-wt-24h) maintained the original size, shape and appearance (Figure 2b), its N_2 sorption isotherm after immersing in water exhibited a dramatic change from a type I to type IV isotherm, which is typical for a mesoporous material (Figure 2a).[19] The pore-size distribution profile, calculated from the desorption isotherm by the Barrett–Joyner–Halenda (BJH) method, showed two distinct mesopores with a diameter of 3.8 and 13.9 nm (Supporting

Information, Figure S6). Also, this sorption isotherm showed an H1 type hysteresis loop, which is characteristic of well-defined cylindrical pore channels.[19] Furthermore, the total specific pore volume increased (from 0.89 $cm^3 g^{-1}$ to 0.94 $cm^3 g^{-1}$), while the surface area decreased significantly (from 2400 $m^2 g^{-1}$ to 620 $m^2 g^{-1}$) owing to the loss of microporosity and emergence of mesoporosity.

The generation of mesopores in POST-66(Y)-wt-24h was confirmed by various electron microscopic studies. Scanning electron microscopy (SEM) images (Supporting Information, Figure S7) exhibited a dramatic morphology change at the surface of POST-66(Y) after the transformation; the surface was covered with many grooves and voids of nanometer size, whereas a very smooth surface was observed before the transformation. Transmission electron microscopy (TEM) and scanning transmission electron microscopy (STEM) images (Figure 3; Supporting Information, Figure S8) illustrated the development of mesopores with a size mostly within 10 to 20 nm, consistent with the pore size distribution obtained by N_2 sorption analysis. The mesopores are also randomly distributed and interconnected with each other to form three-dimensional mesoporous channels. Despite the generation of mesopores, POST-66(Y)-wt-24h retained the original microporous structure, at least partially, as suggested by both single-crystal and powder X-ray diffraction studies (Supporting Information, Figure S10). Although the intensity was significantly reduced, the remaining diffraction peaks at the low θ region matched well the original unit cell of POST-66(Y). Moreover, the Lewis acidic sites of POST-66(Y) were partially preserved in POST-66(Y)-wt-24h as confirmed by in situ IR spectroscopy using acetonitrile as a probe molecule (Supporting Information, Figure S11).[21]

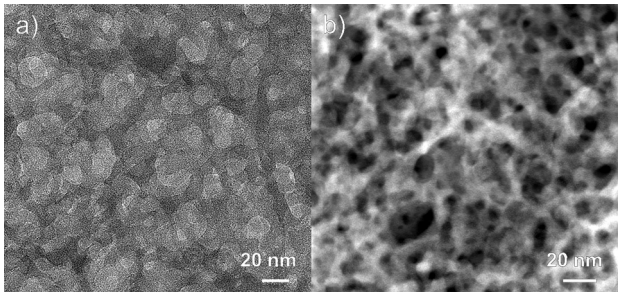

Figure 3. Electron microscopy images of POST-66(Y) after soaking in water a) TEM, b) STEM images of POST-66(Y)-wt-24h.

For a better understanding of the water-induced structural transformation, the process was monitored at a regular interval for 24 h. A series of N_2 adsorption and desorption isotherms for the water treated sample (POST-66(Y)-wt) revealed interesting changes in porosity. First, as time goes by, a gradual loss of micropores and concomitant emergence of mesopores were observed (Figure 4; Supporting Information, Figure S12, S13). As a result, the micropore volume decreased while the mesopore volume increased (Supporting Information, Table S1 and Figure S14). Further careful inspection of the pore size distribution profiles revealed that: 1) the loss of micropores occurred mostly within an hour and little change in microporosity was observed afterwards (see the first slope at low P/P_0 in Figure 4a; Supporting Information, Figure S12); 2) mesopores of 3–4 nm in size are generated rapidly during the first 5–10 min; and 3) after that, a slow evolution of the mesopores occurs until 24 h: 3–4 nm mesopores decrease while over 10 nm mesopores increase (Figure 4b; Supporting Information, Figure S13). A series of PXRD profiles taken during the hydrolytic transformation (Figure 4c) confirmed the maintenance of the original microporous structure, at least in part, during the mesopore generation.

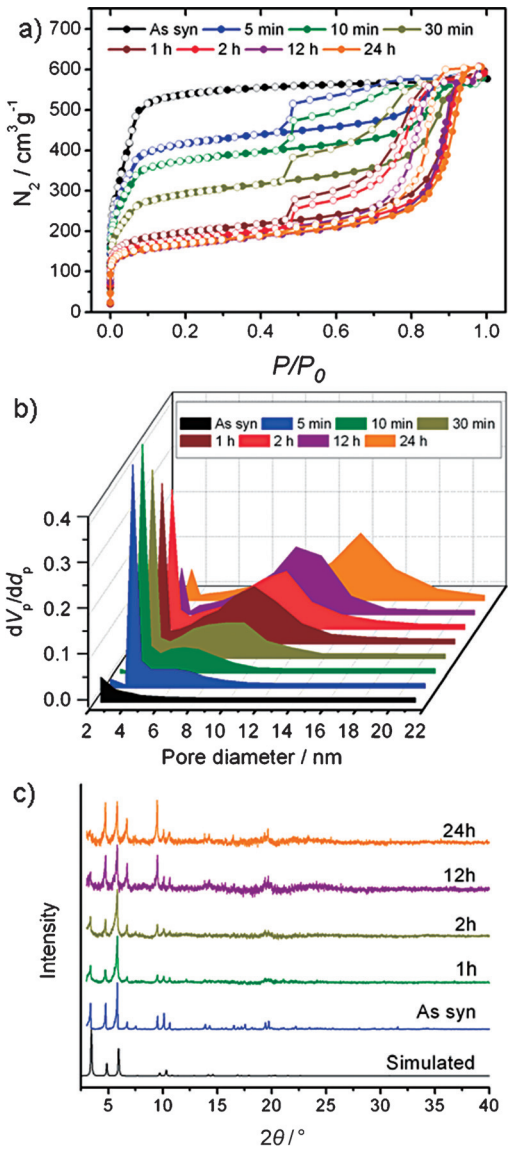

Figure 4. a) N_2 sorption isotherms, b) pore distribution profiles, and c) PXRD patterns of POST-66(Y) after soaking in water at room temperature for different periods of time.

During the hydrolytic transformation of POST-66(Y), both metal ion and ligand constituting the framework were expected to be leached out from the MOF. The leaching of metal ions and ligand was monitored by ICP-AES and UV/Vis spectroscopy, respectively. As shown in the Supporting

Information, Figure S15, leaching of yttrium ions occurred rapidly upon water treatment; approximately 19% of yttrium ions of POST-66(Y) were leached out within 1 h and much slower leaching was observed afterwards. Surprisingly, however, almost no hmtt ligand was leached out (< 0.1%) during the water treatment. It is also interesting to note that the kinetic profile of the metal leaching is in parallel with that of the reduction of micropore volumes observed by N_2 sorption experiments (Supporting Information, Figure S16).

Taken together, these results suggest that the microporous to mesoporous transformation of POST-66(Y) proceeds in two stages (Supporting Information, Figure S17). The first stage involves the dissolution of yttrium ions from the MOF, which results in the formation of mesopores with a size of 3–4 nm at the loss of micropores. In the second stage, the reorganization of yttrium ions and hmtt ligands at the surface of the newly formed mesopores leads to the further growth into a size over 10 nm; at the same time, the formation of a new amorphous phase occurs at the mesopore surface, which prevents further leaching of yttrium ions, as indicated by little loss of yttrium after 1 h (Supporting Information, Figure S15). The structure of the new amorphous phase at the molecular level is not clear yet, and needs further investigations.

When the temperature for the water treatment increased to 80 °C, the microporous-to-mesoporous transformation proceeded more rapidly (Supporting Information, Figure S18a). For example, a 10 min water treatment at 80 °C generated mesopores of 12 nm, which is even larger than those formed by 12 h treatment at room temperature. Further treatment with water for 12 h at 80 °C produced even larger mesopores in the range of 16 ± 5 nm (Supporting Information, Figure S18b). Similar transformations were also observed in isostructural MOFs with lanthanide metal ions such as POST-66(Dy/Tb) (Supporting Information, Figure S20). The *meso*-MOF(Tb)[7b] also underwent a similar transformation to produce much larger mesopores, in the range of 24 to 38 nm (Supporting Information, Figure S21). Preliminary results suggest that the hydrolytic transformation is applicable to other well-known MOFs including MOF-177, UiO-67, and MIL-100 (Supporting Information, Figures S22, S24, and S25, respectively) if we carefully control the hydrolysis conditions such as pH, temperature, time, and water content of mixed solvents. Further work is in progress to expand the scope of this approach.

The mesoporosity of POST-66(Y)-wt can be utilized to immobilize large guest molecules such as proteins and enzymes, which are too large to be immobilized in conventional microporous MOFs. Encapsulation of several guest molecules, including vitamin B_{12}, cytochrome *c*, myoglobin, and horseradish peroxidase in POST-66(Y)-wt-24h was studied by UV/Vis spectroscopy (Table 1; Supporting Information, Figure S27). After encapsulation, the colorless POST-66(Y)-wt-24h turned to red or orange color, confirming successful encapsulation of the guests, while POST-66(Y) showed no color change even after soaking in vitamin B_{12} solution (Supporting Information, Figures S28, S29).

After the successful encapsulation, we investigated the catalytic activity of horseradish peroxidase (HRP) embedded in POST-66(Y)-wt-24h (HRP@POST-66(Y)-wt-24h) on co-oxidation of 4-aminoantiprine (4-AAP) and phenol to *N*-antipyryl-*p*-benzoquinoeimine (APBQ) (Figure 5). The reaction was monitored by following the product formation by UV/Vis spectroscopy. HRP@POST-66(Y)-wt-24h catalyzed the reaction with a reaction rate of 6.94×10^{-5} mmol L s^{-1}, while no activity was observed for POST-66(Y)-wt-24h (Figure 5b; Supporting Information, Table S2). When HRP@POST-66(Y)-wt-24h was removed by filtration after 5 and 15 min, respectively, there was no further progress in the reaction, indicating little leaching of the enzyme from HRP@POST-66(Y)-wt-24h. HRP@POST-66(Y)-wt-24h could be recycled in several times, with a gradual decrease of the reaction rate to 5.1×10^{-5} mmol L s^{-1} after 5 runs (Supporting Information, Figure S31). Furthermore, when the reaction was performed in the presence of organic solvents such as DMSO, HRP@POST-66(Y)-wt-24h showed a better stability than the free HRP (Supporting Information, Figure S33). These results suggest that POST-66(Y)-wt can be utilized as a solid support for immobilization of enzymes to achieve the better stability and recyclability.

In summary, we presented a new approach to the construction of hierarchical micro- and mesoporous MOFs from microporous MOFs by a hydrolytic process. The size of pores can be controlled by modulating the hydrolysis time and temperature. The dimension of the mesopores generated by this method can be as large as 20 nm, which is rather difficult

Table 1: Inclusion of guest molecules in POST-66(Y)-wt-24h.[a]

Guest	Size [nm)]	Solution	Loading [μmol g^{-1}]
VB_{12}	1.0 × 1.6 × 1.7	MeOH	16.1
Cyt *c*	2.6 × 3.2 × 3.3	HEPES buffer[b]	11.8
myoglobin	2.1 × 3.5 × 4.4	HEPES buffer[b]	9.4
HRP	4.0 × 4.4 × 6.8	HEPES buffer[b]	0.42

[a] VB_{12} = Vitamin B_{12}, Cyt *c* = cytochrome *c*, HRP = horseradish peroxidase. [b] 10 mM, pH 7.4.

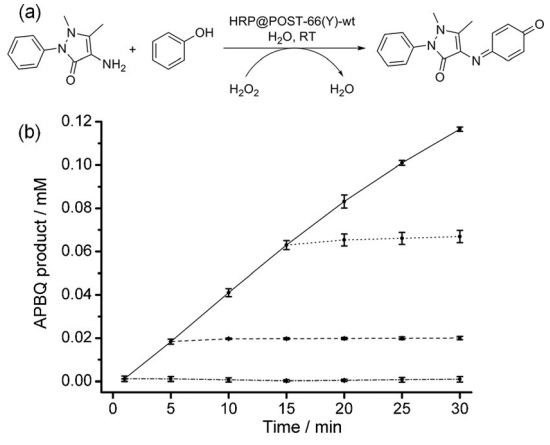

Figure 5. a) Co-oxidation of 4-AAP and phenol to APBQ, b) Kinetic traces of the reaction carried out with POST-66(Y)-wt-24h (–•–•) and HRP@POST-66(Y)-wt-24h (——, •••••, -----); the latter two lines represent the situation where the catalyst was removed after 5 (•••••) and 15 min (-----) of the reaction.

to obtain by conventional MOF syntheses. Moreover, this method does not require an elaborated synthetic procedure to produce mesopores unlike other methods. This simple method is also applicable to other MOFs. Furthermore, the efficient encapsulation of an enzyme in the resulting hierarchical micro- and mesoporous MOF with enhanced enzyme stability and recyclability has also been demonstrated. This approach may provide an exciting opportunity to synthesize new hierarchical porous MOFs with interesting properties for various applications.

Acknowledgements

This work was supported by Institute for Basic Science (IBS) [IBS-R007-D1]. X-ray diffraction experiment with synchrotron radiation was performed at the Pohang Accelerator Laboratory (Beamline 2D).

Keywords: hierarchical porosity · mesoporous materials · metal–organic frameworks · post-synthetic transformation · protein immobilization

How to cite: *Angew. Chem. Int. Ed.* **2015**, *54*, 13273–13278
Angew. Chem. **2015**, *127*, 13471–13476

[1] a) M. P. Suh, H. J. Park, T. K. Prasad, D.-W. Lim, *Chem. Rev.* **2012**, *112*, 782–835; b) K. Sumida, D. R. Rogow, J. A. Mason, T. M. McDonald, E. D. Bloch, Z. R. Herm, T.-H. Bae, J. R. Long, *Chem. Rev.* **2012**, *112*, 703–723; c) Y. He, W. Zhou, G. Qian, B. Chen, *Chem. Soc. Rev.* **2014**, *43*, 5657–5678.

[2] a) E. D. Bloch, W. L. Queen, R. Krishna, J. M. Zadrozny, C. M. Brown, J. R. Long, *Science* **2012**, *335*, 1606–1610; b) J.-R. Li, J. Sculley, H.-C. Zhou, *Chem. Rev.* **2012**, *112*, 869–932; c) B. Van de Voorde, B. Bueken, J. Denayer, D. D. Vos, *Chem. Soc. Rev.* **2014**, *43*, 5766–5788.

[3] a) J. Lee, O. K. Farha, J. Roberts, K. A. Scheidt, S. T. Nguyen, J. T. Hupp, *Chem. Soc. Rev.* **2009**, *38*, 1450–1459; b) M. Yoon, R. Srirambalaji, K. Kim, *Chem. Rev.* **2012**, *112*, 1196–1231; c) A. Dhakshinamoorthy, H. Garcia, *Chem. Soc. Rev.* **2014**, *43*, 5750–5765; d) T. Zhang, W. Lin, *Chem. Soc. Rev.* **2014**, *43*, 5982–5993; e) J. Liu, L. Chen, H. Cui, J. Zhang, L. Zhang, C.-Y. Su, *Chem. Soc. Rev.* **2014**, *43*, 6011–6061.

[4] a) K. M. L. Taylor-Pashow, J. D. Rocca, Z. Xie, S. Tran, W. Lin, *J. Am. Chem. Soc.* **2009**, *131*, 14261–14263; b) P. Horcajada, T. Chalati, C. Serre, B. Gillet, C. Sebrie, T. Baati, J. F. Eubank, D. Heurtaux, P. Clayette, C. Kreuz, J.-S. Chang, Y. K. Hwang, V. Marsaud, P.-N. Bories, L. Cynober, S. Gil, G. Férey, P. Couvreur, R. Gref, *Nat. Mater.* **2010**, *9*, 172–178; c) P. Horcajada, R. Gref, T. Baati, P. K. Allan, G. Maurin, P. Couvreur, G. Férey, R. E. Morris, C. Serre, *Chem. Rev.* **2012**, *112*, 1232–1268.

[5] a) L. E. Kreno, K. Leong, O. K. Farha, M. Allendorf, R. P. Van Duyne, J. T. Hupp, *Chem. Rev.* **2012**, *112*, 1105–1125; b) Z. Hu, B. J. Deibert, J. Li, *Chem. Soc. Rev.* **2014**, *43*, 5815–5840; c) P. Ramaswamy, N. E. Wong, G. K. H. Shimizu, *Chem. Soc. Rev.* **2014**, *43*, 5913–5932; d) P. Falcaro, R. Ricco, C. M. Doherty, K. Liang, A. J. Hill, M. J. Styles, *Chem. Soc. Rev.* **2014**, *43*, 5513–5560.

[6] a) M. Eddaoudi, J. Kim, D. T. Vodak, A. C. Sudik, J. Wachter, M. O'Keeffe, O. M. Yaghi, *Proc. Natl. Acad. Sci. USA* **2002**, *99*, 4900–4904; b) J. J. Perry IV, J. A. Perman, M. J. Zaworotko, *Chem. Soc. Rev.* **2009**, *38*, 1400–1417; c) M. O'Keeffe, O. M. Yaghi, *Chem. Rev.* **2012**, *112*, 675–702; d) W. Lu, Z. Wei, Z.-Y. Gu, T.-F. Liu, J. Park, J. Park, J. Tian, M. Zhang, Q. Zhang, T. Gentle III, M. Bosch, H.-C. Zhou, *Chem. Soc. Rev.* **2014**, *43*, 5561–5593.

[7] a) X.-S. Wang, S. Ma, D. Sun, S. Parkin, H.-C. Zhou, *J. Am. Chem. Soc.* **2006**, *128*, 16474–16475; b) Y. K. Park, S. B. Choi, H. Kim, K. Kim, B.-H. Won, K. Choi, J.-S. Choi, W.-S. Ahn, N. Won, S. Kim, D. H. Jung, S.-H. Choi, G.-H. Kim, S.-S. Cha, Y. H. Jhon, J. K. Yang, J. Kim, *Angew. Chem. Int. Ed.* **2007**, *46*, 8230–8233; *Angew. Chem.* **2007**, *119*, 8378–8381; c) K. Koh, A. G. Wong-Foy, A. J. Matzger, *Angew. Chem. Int. Ed.* **2008**, *47*, 677–680; *Angew. Chem.* **2008**, *120*, 689–692; d) H. Furukawa, N. Ko, Y. B. Go, N. Aratani, S. B. Choi, E. Choi, A. O. Yazaydin, R. Q. Snurr, M. O'Keeffe, J. Kim, O. M. Yaghi, *Science* **2010**, *329*, 424–428; e) W. Xuan, C. Zhu, Y. Liu, Y. Cui, *Chem. Soc. Rev.* **2012**, *41*, 1677–1695.

[8] D. Bradshaw, S. El-Hankari, L. Lupica-Spagnolo, *Chem. Soc. Rev.* **2014**, *43*, 5431–5443.

[9] a) H. Deng, S. Grunder, K. E. Cordova, C. Valente, H. Furukawa, M. Hmadeh, F. Gándara, A. C. Whalley, Z. Liu, S. Asahina, H. Kazumori, M. O'Keeffe, O. Terasaki, J. F. Stoddart, O. M. Yaghi, *Science* **2012**, *336*, 1018–1023; b) D. Feng, T.-F. Liu, J. Su, M. Bosch, Z. Wei, W. Wan, D. Yuan, Y.-P. Chen, X. Wang, K. Wang, X. Lian, Z.-Y. Gu, J. Park, X. Zou, H.-C. Zhou, *Nat. Commun.* **2015**, *6*, 5979.

[10] a) L.-G. Qiu, T. Xu, Z.-Q. Li, W. Wang, Y. Wu, X. Jiang, X.-Y. Tian, L.-D. Zhang, *Angew. Chem. Int. Ed.* **2008**, *47*, 9487–9491; *Angew. Chem.* **2008**, *120*, 9629–9633; b) Y. Zhao, J. Zhang, B. Han, J. Song, J. Li, Q. Wang, *Angew. Chem. Int. Ed.* **2011**, *50*, 636–639; *Angew. Chem.* **2011**, *123*, 662–665; c) L.-B. Sun, J.-R. Li, J. Park, H.-C. Zhou, *J. Am. Chem. Soc.* **2012**, *134*, 126–129; d) J. Reboul, S. Furukawa, N. Horike, M. Tsotsalas, K. Hirai, H. Uehara, M. Kondo, N. Louvain, O. Sakata, S. Kitagawa, *Nat. Mater.* **2012**, *11*, 717–723.

[11] a) J. Park, Z. U. Wang, L.-B. Sun, Y.-P. Chen, H.-C. Zhou, *J. Am. Chem. Soc.* **2012**, *134*, 20110–20116; b) H. Wu, Y. S. Chua, V. Krungleviciute, M. Tyagi, P. Chen, T. Yildirim, W. Zhou, *J. Am. Chem. Soc.* **2013**, *135*, 10525–10532; c) G. Barin, V. Krungleviciute, O. Gutov, J. T. Hupp, T. Yildirim, O. K. Farha, *Inorg. Chem.* **2014**, *53*, 6914–6919; d) Z. Fang, J. P. Dürholt, M. Kauer, W. Zhang, C. Lochenie, B. Jee, B. Albada, N. Metzler-Nolte, A. Pöppl, B. Weber, M. Muhler, Y. Wang, R. Schmid, R. A. Fischer, *J. Am. Chem. Soc.* **2014**, *136*, 9627–9636.

[12] a) M. R. Lohe, M. Rose, S. Kaskel, *Chem. Commun.* **2009**, 6056–6058; b) Y. Yue, Z.-A. Qiao, P. F. Fulvio, A. J. Binder, C. Tian, J. Chen, K. M. Nelson, X. Zhu, S. Dai, *J. Am. Chem. Soc.* **2013**, *135*, 9572–9575; c) L. Li, S. Xiang, S. Cao, J. Zhang, G. Ouyang, L. Chen, C.-Y. Su, *Nat. Commun.* **2013**, *4*, 1774; d) L. Peng, J. Zhang, Z. Xue, B. Han, X. Sang, C. Liu, G. Yang, *Nat. Commun.* **2014**, *5*, 5465.

[13] a) K. K. Tanabe, Z. Wang, S. M. Cohen, *J. Am. Chem. Soc.* **2008**, *130*, 8508–8517; b) S. M. Cohen, *Chem. Rev.* **2012**, *112*, 970–1000.

[14] a) S. Das, H. Kim, K. Kim, *J. Am. Chem. Soc.* **2009**, *131*, 3814–3815; b) Y. Kim, S. Das, S. Bhattacharya, S. Hong, M. G. Kim, M. Yoon, S. Natarajan, K. Kim, *Chem. Eur. J.* **2012**, *18*, 16642–16648; c) B. J. Burnett, P. M. Barron, C. Hu, W. Choe, *J. Am. Chem. Soc.* **2011**, *133*, 9984–9987; d) M. Kim, J. F. Cahill, Y. Su, K. A. Prather, S. M. Cohen, *Chem. Sci.* **2012**, *3*, 126–130; e) O. Karagiaridi, W. Bury, J. E. Mondloch, J. T. Hupp, O. K. Farha, *Angew. Chem. Int. Ed.* **2014**, *53*, 4530–4540; *Angew. Chem.* **2014**, *126*, 4618–4628; f) C. K. Brozek, M. Dinca, *Chem. Soc. Rev.* **2014**, *43*, 5456–5467; g) P. Deria, J. E. Mondloch, O. Karagiaridi, W. Bury, J. T. Hupp, O. K. Farha, *Chem. Soc. Rev.* **2014**, *43*, 5896–5912.

[15] a) V. Valtchev, G. Majano, S. Mintova, J. Pérez-Ramírez, *Chem. Soc. Rev.* **2013**, *42*, 263–290; b) I. I. Ivanova, E. E. Knyazeva, *Chem. Soc. Rev.* **2013**, *42*, 3671–3688; c) D. P. Serrano, J. M. Escola, P. Pizarro, *Chem. Soc. Rev.* **2013**, *42*, 4004–4035.

[16] B. Tu, Q. Pang, D. Wu, Y. Song, L. Weng, Q. Li, *J. Am. Chem. Soc.* **2014**, *136*, 14465 – 14471.
[17] http://rcsr.anu.edu.au/nets/reo.
[18] Void space and density are calculated with framework structure of POST-66(Y) from the X-ray analysis using PLATON software: a) A. L. Spek, *Acta Crystallogr. Sect. A* **1990**, *46*, C34; b) A. L. Spek, PLATON, A Multipurpose Crystallographic Tool, Utrecht University, Utrecht, **1998**.
[19] a) K. S. W. Sing, D. H. Everett, R. A. W. Haul, L. Moscou, R. A. Pierotti, J. Rouquérol, T. Siemieniewska, *Pure Appl. Chem.* **1985**, *57*, 603 – 619; b) P. Schneider, *Appl. Catal. A* **1995**, *129*, 157 – 165.
[20] a) K. Tan, N. Nijem, P. Canepa, Q. Gong, J. Li, T. Thonhauser, Y. J. Chabal, *Chem. Mater.* **2012**, *24*, 3153 – 3167; b) J. J. Low, A. I. Benin, P. Jakubczak, J. F. Abrahamian, S. A. Faheem, R. R. Willis, *J. Am. Chem. Soc.* **2009**, *131*, 15834 – 15842.
[21] F. Vermoortele, B. Bueken, G. Le Bars, B. Van de Voorde, M. Vandichel, K. Houthoofd, A. Vimont, M. Daturi, M. Waroquier, V. Van Speybroeck, C. Kirschhock, D. E. De Vos, *J. Am. Chem. Soc.* **2013**, *135*, 11465 – 11468.

Received: July 11, 2015
Revised: August 20, 2015
Published online: September 18, 2015

